Proceedings World Geothermal Congress 2020+1
Reykjavik, Iceland, April - October 2021

Theoretical and Experimental Study of the Thermal and Dielectric Properties of Loess Soils

Henok Hailemariam and Frank Wuttke; Thomas Schicht and Sandro John

Geomechanics and Geotechnics, Kiel University, Kiel, Germany

henok.hailemariam@ifg.uni-kiel.de, frank.wuttke@ifg.uni-kiel.de

Keywords: Effective thermal conductivity; effective complex dielectric permittivity, moisture content, loess soils.

ABSTRACT

Thermal conductivity plays a vital role in the conductive heat transfer analysis of many engineering applications, such as the operation of small and large scale seasonal thermal energy storage, energy transport and geothermal energy systems. Hence, accurate and fast determination of the effective thermal conductivity of geomaterials (heat storage media) at single points or as a spatial plane images is vital in the design and operation of such systems. For solid sensible heat storage materials, the heat storage medium can vary from cemented porous media to a wide variety of natural soils. Besides exiting laboratory and field measurement techniques, one promising approach, which can be used to accurately estimate the effective thermal conductivity of large-scale porous media deposits is via the application of dielectric data measurements (such as complex dielectric permittivity) by using non-destructive high frequency electromagnetic (HF-EM) techniques such as ground penetrating radar (GPR). For this application to work, having a strong correlation between the two controlling heat transfer and electromagnetic parameters (i.e. effective thermal conductivity and effective complex dielectric permittivity, respectively) is necessary. In this study, the variations of the effective thermal conductivity and effective complex dielectric permittivity of a loess soil with moisture content are investigated theoretically and experimentally by performing transient thermal conductivity and HF-EM tests. The results show a strong correlation between the two parameters, indicating the possibility of using dielectric measurements for obtaining effective thermal conductivity of loess soils.

1. INTRODUCTION

The effective thermal conductivity and effective complex dielectric permittivity of soils are highly correlated and are both affected by the changes in chemical composition, grain structure and hydro-mechanical conditions. The findings of several studies on the behavior of effective thermal conductivity and effective dielectric permittivity of soils carried out in the past (Fragkogiannis et al., 2010; Hailemariam et al., 2017; Hailemariam, 2019), confirm the strong correlation between the two parameters. Considering the current limitations on the availability of large scale sub-surface thermal exploration (measurement) techniques, the use of large scale non-destructive HF-EM sub-surface measurement techniques, such as GPR, to obtain soil dielectric properties which can then be correlated to their thermal properties, provide a promising alternative (Hailemariam et al., 2017; Hailemariam, 2019). In order to develop such accurate thermal behavior prediction or correlation models from dielectric behavior, a strong correlation between the thermal and dielectric properties of the desired soils should be established first. To this regard, in this study, the variations of the effective thermal conductivity and effective complex dielectric permittivity of a loess soil with moisture content are analyzed theoretically and experimentally, and the correlation between the two parameters is discussed.

2. THEORETICAL ANALYSIS

2.1 Structure of Soils

Naturally occurring unsaturated soils typically contain four phases, namely solid grains, free and bound water, air and contractile skin (or air-water interface) (Fredlund and Morgenstern, 1977). Soils which commonly exhibit these phases in unsaturated state are the natural, desiccated soils and compacted soils. The effective thermal and dielectric properties of such soils are usually expressed as a sum or equivalent of the contributions of the individual constituent phases based on their volumetric or weight proportions. The thermal and dielectric properties of the bound water phase of porous media are poorly understood and difficult to quantify, and hence are generally neglected for practical purposes (Wagner and Scheuermann, 2009; Hailemariam et al., 2017).

2.2 Dielectric Behavior

The broadband effective electromagnetic transfer functions ε^*_{eff} or σ^*_{eff} of the porous medium can be introduced by assuming the dependence of complex electrical conductivity σ^* and complex dielectric permittivity ε^* on frequency $\omega = 2\pi f$. In addition to the frequency, these transfer functions are also dependent on the thermodynamic state parameters such as temperature, pressure, saturating fluid content etc. (Jonscher, 1977).

The effective complex absolute permittivity ε^*_{eff} (F m^{-1}) is represented as:

$$\varepsilon^*_{eff} = \varepsilon'_{eff} - j\varepsilon''_{eff} = \varepsilon_0(\varepsilon'_{r,eff} - j\varepsilon''_{r,eff}) \tag{1}$$

with the effective complex absolute electrical conductivity σ^*_{eff} (S m^{-1}) represented as:

$$\sigma^*_{eff} = j\omega\varepsilon^*_{eff} \tag{2}$$

and the relative effective complex magnetic permeability $\mu^*_{r,eff}$ represented as:

$$\mu^*_{r,eff} = \frac{\mu^*_{eff}}{\mu_0} \tag{3}$$

where, ε_0 = 8.854187817 × 10^{-12} F m^{-1} and $\mu_0 = 4\pi \times 10^{-7}$ or 1.2566370614 × 10^{-6} H m^{-1} are the permittivity and magnetic permeability of free space, respectively. For most soils, the presence of iron content is negligible and the constituent phases are considered non magnetizable, consequently, the relative magnetic permeability is set to 1 (i.e. magnetic effects are neglected). The relative effective complex permittivity $\varepsilon^*_{r,eff} = \varepsilon'_{r,eff} - j\varepsilon''_{r,eff}$ has two components, where the real part $\varepsilon'_{r,eff}$ represents the amount of energy stored in the material when it is exposed to an electromagnetic field (Lauer et al., 2012). Whereas, the imaginary part $\varepsilon''_{r,eff} = \varepsilon''_{r,d} + \sigma_{DC}/(\omega\varepsilon_0)$ (σ_{DC}, S m^{-1}, is the direct current conductivity) represents the Ohmic and polarization losses (the displacement of the randomly orientated and non-polarized electrical charges in a dielectric relative to each other in order to compensate for an applied electric field leading to a polarized medium) (Hasted, 1973).

The equivalent or effective relative complex permittivity of a soil can be expressed in terms of the individual dielectric permittivities of the constituent phases using theoretical formulations such as the volume fraction (VF) model (Lichtenecker and Rother, 1931). In this study, the VF model (Equations 4 and 5) is selected to model the dielectric behavior of the loess soil due to its simple structure and wide range of application.

$$\varepsilon^{*a}_{r,eff} = V_s\varepsilon^{*a}_{r,g} + V_a\varepsilon^{*a}_{r,a} + V_w\varepsilon^{*a}_{r,w} \tag{4}$$

$$\varepsilon'^{a}_{r,eff} = (1-n)\varepsilon'^{a}_{r,g} + (n-\theta) + \theta\varepsilon'^{a}_{r,w} \tag{5}$$

where, V_s, V_a and V_w are the volumetric fractions of the solids, pore-air and pore-water constituent phases of the soil, respectively, n is the porosity of the soil, θ is the volumetric water content of the soil, $\varepsilon^*_{r,eff}$ is the relative effective complex permittivity of the soil, $\varepsilon^*_{r,g} = (1.01 + 0.44G_s)^2 - 0.062$ (Dobson et al., 1985), $\varepsilon^*_{r,a}$ and $\varepsilon^*_{r,w}$ are the relative complex dielectric permittivities of the solid grains, pore-air and pore-water constituent phases of the soil, respectively, structural exponent a = 1/2 (complex refractive index model or CRIM) (Birchak et al., 1974), $\varepsilon'_{r,eff}$ is the real part of the relative effective complex permittivity of the soil, $\varepsilon'_{r,g}$, $\varepsilon'_{r,a}$ and $\varepsilon'_{r,w}$ are the real parts of the relative complex dielectric permittivities of the solid grains, pore-air and pore-water constituent phases of the soil, respectively, and G_s is the specific gravity of the solid particles.

The electromagnetic behavior of the solid phases (grains) and pore-air of most soils show minor variations with changes in frequency and temperature, and hence can be assumed to be frequency and temperature independent. Whereas, the pore-water phase is an aqueous solution which is highly sensitive to both frequency and temperature changes. The complex permittivity of the water molecules as a function of frequency is determined by their polarizability and dielectric losses, and their dielectric spectrum can be described by the modified Debye model, which for single-phased homogeneous materials such as pure water is represented as follows (Asami, 2002; Wagner and Scheuermann, 2009) (Figure 1):

$$\varepsilon^*_{r,w}(\omega,T) = \varepsilon_\infty(T) + \frac{\Delta\varepsilon(T)}{1+j\omega\tau_w(T)} - j\frac{\sigma_{DC}(T)}{\omega\varepsilon_0} \tag{6}$$

where, $\varepsilon^*_{r,w}$ is the frequency and temperature dependent relative complex dielectric permittivity of water, ε_∞ is the temperature dependent high frequency limit of permittivity, $\Delta\varepsilon = \varepsilon_s - \varepsilon_\infty$ is the temperature dependent relaxation magnitude, ε_s is the temperature dependent static permittivity, $j = \sqrt{-1}$ is the imaginary unit, $\omega = 2\pi f$ (rad) is the angular frequency, τ_w (s) is the temperature dependent relaxation time of water, σ_{DC} (S m^{-1}) is the temperature dependent direct current conductivity.

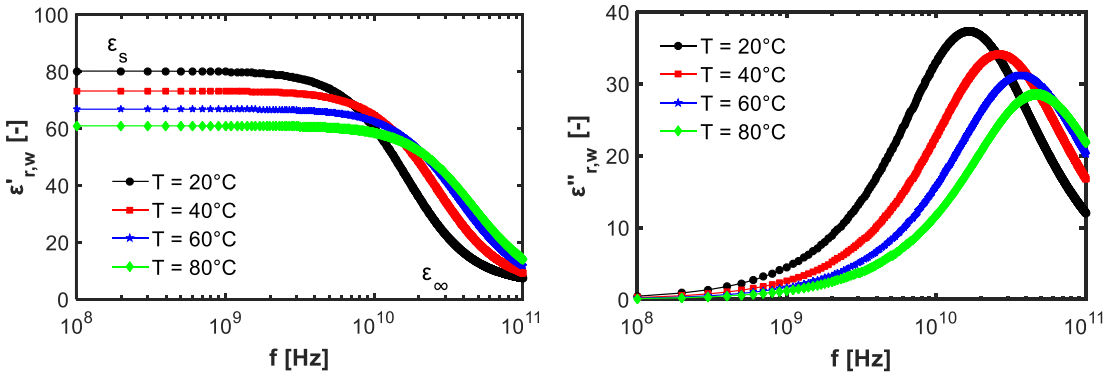

Figure 1: Dielectric spectra of water according to the modified Debye model (Equation 6) with the real $\varepsilon'_{r,eff}$ (left) and imaginary $\varepsilon''_{r,eff}$ (right) parts of the relative complex dielectric permittivity.

2.3 Thermal Behavior

Laboratory or field-scale experimental techniques for the precise determination of the effective thermal conductivity of soils are difficult and usually time-consuming to conduct. Hence, several researchers have suggested models relating the effective thermal conductivity of soils to readily obtainable parameters such as moisture content, porosity, temperature, mineral content, pressure etc. (Kersten, 1949). In a typical three-phase soil system of solid particles, pore-air and pore-water, the apparent or effective thermal conductivity of the resulting mix is a function of the air and water content (Bristow, 2002). In this study, the effective thermal conductivity of the loess soil is modeled using the modified form of the Johansen's semi-empirical equation of thermal conductivity (Equation 7) (Johansen, 1975; Hailemariam et al., 2017), due to its simplicity and accuracy of prediction.

$$\lambda = (\lambda_{sat} - \lambda_d)\frac{\kappa(\theta/n)}{1+(\kappa-1)(\theta/n)} + \lambda_d \tag{7}$$

$$\lambda_d = \frac{0.135\rho_d + 64.7}{\rho_s - 0.947\rho_d} \quad (8)$$

$$\lambda_{sat} = \lambda_s{}^{1-n}\lambda_w{}^{n} \quad (9)$$

where, λ (W m^{-1} K^{-1}) is the three-phase effective thermal conductivity of the soil, λ_d and λ_{sat} (W m^{-1} K^{-1}) are the dry and saturated bulk thermal conductivities of the soil, λ_s and λ_w (W m^{-1} K^{-1}) are the thermal conductivities of the solids and pore-water constituent phases of the soil, respectively, ρ_d and ρ_s (kg m^{-3}) are the bulk dry and solid particle densities of the soil and κ is the soil texture dependent parameter of Côté and Konrad (2005) model.

3. EXPERIMENTAL PROGRAM

3.1 Tested Soil

A remolded loess soil (Figure 2) taken from near Baku area, Azerbaijan, was investigated. The obtained geotechnical properties of the loess soil are provided in Table 1.

Figure 2: A sample of the loess soil.

Table 1. Geotechnical properties of the investigated loess soil

Properties	**Value**
Depth (m)	2.0 – 2.5
Gravel, > 2 mm (wt.%)	0
Sand, 0.063 - 2 mm (wt.%)	15
Silt, 0.002 - 0.063 mm (wt.%)	51
Clay, < 0.002 mm (wt.%)	34
Porosity n (-)	0.453
Solids specific gravity G_s (-)	2.735
Bulk dry density ρ_d (kg m^{-3})	1495
Liquid limit L_L (%)	31.3
Plasticity index P_I (%)	14.3
Natural gravimetric water content w_n (-)	0.093
Unified soil classification system (USCS)	CL

CL: Clay of low plasticity

3.2 Equipments Used

3.2.1 Determination of the Effective Complex Dielectric Spectra of the Loess Soil

The broadband dielectric measurements were performed in the stable frequency range from 100 MHz to 10 GHz at room temperature and atmospheric pressure by means of a time domain reflectometry (TDR) technique with an open ended coaxial line (Wagner et al., 2011). A probe with dia. of 2.2 mm and length of 175 mm connected via a coaxial cable to a Sequid STDR-65 device (Figure 3) was used for the measurements. The resolution of the STDR-65 is 10 *ps* and the sampling interval is 50 *ns*. The acquired step-like TDR time-domain curves are pre-processed in the TDR and subsequently transmitted to a laptop computer, which transforms the signals into the frequency domain using the Fast-Fourier Transform (FFT) and carries out the calibration and permittivity calculations.

Figure 3: Portable Sequid STDR-65 device.

Prior to the measurements a two step calibration procedure was performed to minimize errors in measurement resulting from device and setup. Initially, full one port three-term calibration was done mechanically with (Open, Short, 50 Ω-Match or Load) calibration standards following procedure by Rhode & Schwarz N – 50 Ω ZV-Z21. The second stage (permittivity calibration) was then performed by measuring the complex scattering parameter S_{11} of three materials: air, distilled water and a short circuit. Each calibration standard was measured using 10 averages. The calculation of the relative effective complex dielectric permittivity $\varepsilon^*_{r,eff}$ was obtained as shown in Equation 10 (Wagner et al., 2014). The terms c_i in Equation 10 are three temperature and frequency dependent complex calibration parameters obtained from the permittivity calibration and S_{11} is the measured complex reflection coefficient of the soil.

$$\varepsilon^*_{r,eff}(\omega,T) = \frac{c_1(\omega,T)S_{11}(\omega,T) - c_2(\omega,T)}{c_3(\omega,T) - S_{11}(\omega,T)} \tag{10}$$

3.2.2 Determination of the Effective Thermal Conductivity of the Loess Soil

The effective thermal conductivity of the loess soil was measured using a Decagon KD2 Pro thermal needle probe (Figure 4, left), based on transient line source measurement technique in compliance with ASTM D 5334-08 (2008) and IEEE 442 (1981) standards. Thermal needle probe TR-1 (single needle), with length of 100 mm and diameter 2.4 mm (Figure 4, right), was used to measure the effective thermal conductivity of the soil at room temperature and atmospheric pressure conditions, based on Carslaw and Jaeger (1959) and Kluitenberg et al. (1993) line heat source analysis.

Figure 4: Decagon KD2 Pro thermal device (left) and TR-1 single needle probe (right).

The sufficient length to diameter ratio of the probe ensures that conditions for an infinitely long and infinitely thin heating source are met. The measurement error recorded for the specimens was kept well below the 0.015% limit. The KD2 Pro includes a linear heat source and a temperature measuring element with a resolution of 0.001°C, and computes the effective thermal conductivity of the medium with the TR-1 probe using the following relations:

$$\lambda = \frac{Q(\ln t_2 - \ln t_1)}{4\pi(\Delta T_2 - \Delta T_1)} \tag{11}$$

$$\Delta T = -\frac{Q}{4\pi\lambda}\mathrm{Ei}\left[\frac{-r^2}{4Dt}\right] \tag{12}$$

where, Q (W m^{-1}) is the heat application rate, ΔT (K) is the temporal response of the source's temperature, 'Ei' is the exponent integral, r (m) is the distance between the temperature measuring sensor and the heater, t (s) is the elapsed time since the start of heating, and D (m^2 s^{-1}) is the specimen's thermal diffusivity.

3.3 Experimental Procedure

The loess soil was prepared under a remolded loose condition with a porosity of n = 0.453. A soil sample was incrementally wetted from air dry up to saturation by adding controlled amount of distilled water required for each gravimetric water content and was then allowed to equilibrate for 48 hours. From the prepared sample, subsamples were taken for measurements of thermal conductivity and complex dielectric permittivity for each gravimetric water content. The dry density/porosity of each loess soil sample was kept constant for all gravimetric water contents. Care was taken to pack the samples with a homogeneous bulk density (throughout the specimen volume) and to a constant volume, and a total of 22 measurements of effective thermal conductivity and

effective complex dielectric permittivity were taken. The measurements were repeated at least three times for each subsample for verification.

4. RESULTS AND DISCUSSION

In this section, the experimental and theoretical modelling results of the measurement of the thermal and dielectric properties of the loess soil are presented.

4.1 Dielectric Properties

The results of the electromagnetic measurements on the investigated loess soil are shown in Figures 5 and 6. Figure 5 shows the variation of the real part $\varepsilon'_{r,eff}$ of the relative effective complex permittivity of loess soil at a measurement frequency of 1 GHz with gravimetric water content w. The measured $\varepsilon'_{r,eff}$ of the loess soil increases with an increase in moisture content, as for the given porosity of the soil, an increase in moisture content indicates the replacement of air with moisture, which has a much higher complex dielectric permittivity than air.

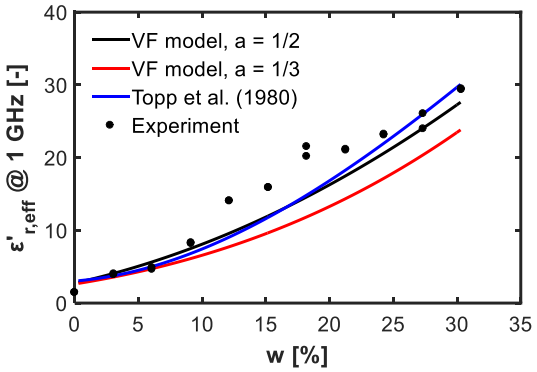

Figure 5: Real part $\varepsilon'_{r,eff}$ of the Relative Effective Complex Permittivity of the Loess Soil as a Function of Water Content w.

Moreover, in Figure 5, the experimental findings are compared to the VF model (Equation 5), with structural exponents a = 1/2 (CRIM) (Birchak et al., 1974) and a = 1/3 (LLLM) (Landau and Lifschitz, 1985), as well as the Topp et al. (1980) model. Although all the models tend to underestimate the measured $\varepsilon'_{r,eff}$ data, the VF model with exponent a = 1/2 and the Topp et al. model match comparatively well with the experimental results as compared to the VF model with exponent a = 1/3, which tends to significantly underestimate the measured $\varepsilon'_{r,eff}$ at 1 GHz data for the whole range of the loess soil saturation.

In Figure 6, the measured dielectric spectra of the relative effective complex permittivity $\varepsilon^*_{r,eff}$ of the loess soil at different gravimetric water contents w is presented. At frequencies above 4 GHz, a low accuracy of signal measurements were recorded for all the samples, possibly due to a limitation in the dynamic range of the employed TDR instrument and radiation effects. Generally, the loess soil exhibits a very high degree of dielectric dispersion or relaxation, due to the presence of a high proportion of clay minerals with readily dissoluble salts (34.0 wt.%, Table 1) (Arulanandan, 2003; Wagner and Scheuermann, 2009).

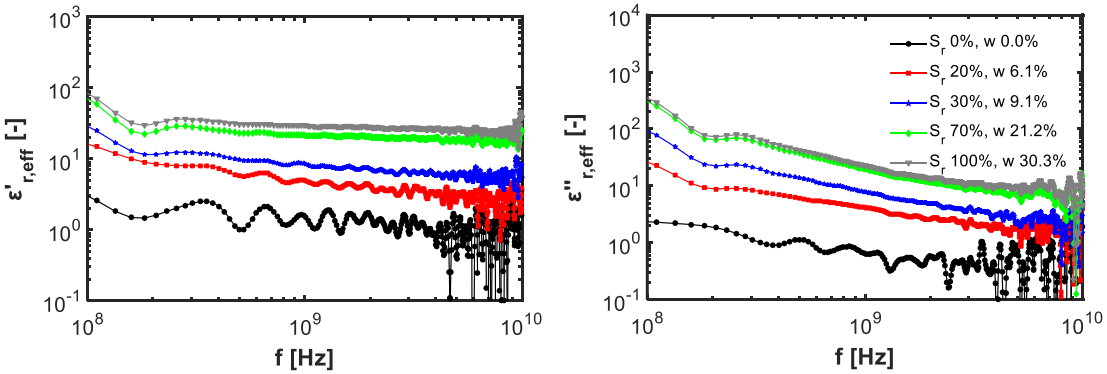

Figure 6: Dielectric Spectra of the Loess Soil Samples at Different Gravimetric Water Contents w: $\varepsilon'_{r,eff}$ (left), and $\varepsilon''_{r,eff}$ (right).

Figure 7 shows the results of effective thermal conductivity λ measurements of the loess soil as a function of gravimetric water content w. Generally, the effective thermal conductivity λ of the loess soil increases with an increase in moisture content in two stages. At gravimetric water content w of up to around 21%, water bridges start to form between the soil particles filling air voids, and λ starts to increase rapidly due to improved contact and increase in heat conduction path between the grains (Sepaskhah and Boersma, 1979). Then after, the increase in λ mainly depends on the replacement of air by water only, and as a result, λ increases at a slower rate.

The experimental findings of λ are further compared to the modified Johansen model (Equation 7), the original Johansen's model (Johansen, 1975) and the Lu etal. (2007) model. All three models match the experimental measurements of λ with good accuracy, except at gravimetric water content w levels below around 7%, where only the modified Johansen model provides a good accuracy (Figure 7). The prediction results of the original Johansen model at low moisture contents are neglected due to its inapplicability for degrees of saturation lower than 20%.

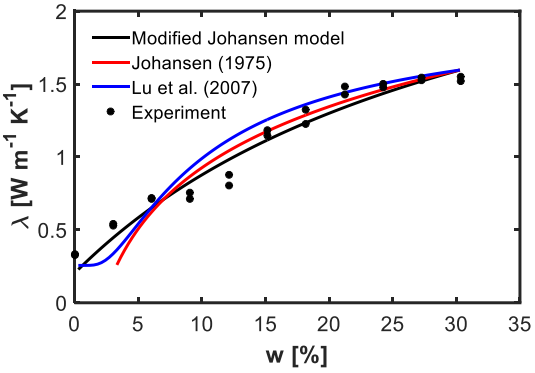

Figure 7: Effective Thermal Conductivity λ of the Loess Soil as a Function of Gravimetric Water Content w.

In summary, moisture content has a similar effect on both the effective dielectric permittivity and effective thermal conductivity of the investigated loess soil. An increase in the values of both effective parameters was recorded with an increase in moisture content of the soil, as for the given soil porosity, an increase in moisture content indicates the replacement of air with moisture, which has a much higher dielectric permittivity and thermal conductivity than air. The results indicate a strong correlation between the two effective parameters in relation to changes in soil moisture content, thus indicating the possibility of inter-prediction of one effective parameter from the other, such as using soil dielectric data from non-destructive geophysical tools to predict effective thermal conductivity of soil deposits at large and small scales.

Despite the strong correlation between the two effective parameters, the results also show that the rate of increase of the two effective parameters with the addition of moisture content is different. Generally, the real $\varepsilon'_{r,eff}$ part of relative effective complex dielectric permittivity at 1 GHz frequency increases slowly at low gravimetric water contents w and with a greater slope at higher w. By contrast, effective thermal conductivity λ increases rapidly at low w, and with a smaller slope at high w. This trend is to be expected, as heat travels through both solid and liquid phases, with even low moisture content forming linkages between soil grains resulting in an early rapid increase of heat conduction and effective thermal conductivity λ. However, the conducting pathway for dielectric permittivity are largely associated to the liquid (pore-water) phase (Hilhorst, 2000). At low gravimetric moisture contents w, the $\varepsilon'_{r,eff}$ of the soil increases slowly because it is mainly associated with water adsorbed on soil colloid particles and forming bridges between the solid grains creating meandering pathways for electrical conductivity. With a further increase in w, the meandering pathways are hugely decreased, and the rapid filling of the voids with pore-water provides a direct path for electrical conduction in the soil, largely enhancing the effective dielectric permittivity or conductivity of the soil.

5. CONCLUSIONS

Assessing the heat transfer behavior of soils is vital in understanding and solving wide variety of problems in the fields of energy geotechnics and engineering. In this regard, accurate determination of the key thermal parameter of soils, i.e. effective thermal conductivity, is of paramount importance. Considering the limitation on the availability and effectiveness of existing thermal conductivity measurement techniques for large scale soil deposits, the use of non-destructive geophysical approaches, such as GPR, to obtain soil dielectric properties at large areas and high depths, which can then be related to its effective thermal conductivity, provides a good and feasible alternative approach. In order to use such approaches, a strong correlation between the effective thermal and dielectric properties of soils should be established first. In this study, the correlation between the effective thermal conductivity and effective complex dielectric permittivity of a loess soil was theoretically and experimentally studied for the whole range of water saturation. The results showed a strong correlation between the two parameters, with both effective parameters increasing with an increase in soil moisture content, mainly due to the replacement of air with moisture (which has a much higher thermal conductivity and dielectric permittivity than air) upon wetting, indicating the possibility of using effective dielectric measurements for obtaining effective thermal conductivity of loess soils in future studies.

ACKNOWLEDGEMENTS

The authors would like to acknowledge the financial support provided by the German Federal Ministry for Economic Affairs and Energy (BMWi) under the Grant numbers 0325547B (Project IGLU) and 03ET6122A (Project ANGUS II) as well as the support of Project Management Jülich. We are also grateful to Ahmed Al-Janabi, University of Babylon, Iraq, for his support in conducting the dielectric measurements.

REFERENCES

Arulanandan, K. (2003). Soil structure: In situ properties and behaviour, Depart. of Civil and Environ. Eng., University of California, Davis, California.

Asami, K. (2002). Characterization of heterogeneous systems by dielectric spectroscopy, *Progress in Polymer Science*, **27 (8)**, 1617-1659.

ASTM D 5334 – 08. (2008). Standard test method for determination of thermal conductivity of soil and soft rock by thermal needle probe procedure, ASTM International, West Conshohocken, Pennsylvania.

Birchak, J., Gardner, C., Hipp, J., and Victor, J. (1974). High dielectric constant microwave probes for sensing soil moisture, *Proceedings of the IEEE*, **62 (1)**, 93-98.

Bristow, K.L. (2002). *Thermal conductivity*, Methods of Soil Analysis Part 4: Physical Methods, SSSA Book Ser. 5, Dane, J.H. and Topp, G.C., Ed., SSSA, Madison, Wisconsin, 1209-1225.

Carslaw, H.S., and Jaeger, J.C. (1959). Conduction of heat in solids, 2nd Ed., Oxford, London, UK.

Côté, J., and Konrad, J.M. (2005). A generalized thermal conductivity model for soils and construction materials, *Canadian Geotechnical Journal*, **42**, 443-458.

Dobson, M.C., Ulaby, F.T., Hallikainen, M.T., and El-Rayes, M.A. (1985). Microwave dielectric behaviour of wet soil - Part II: Dielectric mixing models, *IEEE Transactions on Geoscience and Remote Sensing GE*, **23 (1)**, 35-46.

Fragkogiannis, G., Apostolopoulos, G., and Stamataki, S. (2010). Correlation of thermal conductivity and electrical resistivity of soil - for near surface geothermal applications, 72nd EAGE Conference & Exhibition incorporating SPE EUROPEC 2010, Barcelona, Spain, 3989-3993.

Fredlund, D.G., and Morgenstern, N.R. (1977). Stress state variables for unsaturated soils, *Journal of the Geotechnical Engineering Division*, **103 (5)**, 447-466.

Hailemariam, H. (2019). Thermal and dielectric behavior of porous media, PhD thesis, Faculty of Mathematics and Natural Sciences, Kiel University, Kiel, Germany. (accepted)

Hailemariam, H., Shrestha, D., Wuttke, F., and Wagner, N. (2017). Thermal and dielectric behaviour of fine-grained soils, *Environmental Geotechnics*, **4 (2)**, 79-93.

Hasted, J.B. (1973). *Aqueous dielectrics*, Chapman and Hall, London, UK.

Hilhorst, M.A. (2000). A pore water conductivity sensor, *Soil Science Society of America Journal*, **64 (6)**, 1922-1925.

IEEE 442. (1981). IEEE guide for soil thermal resistivity measurements, Institute of Electrical and Electronics Engineers, New York.

Johansen, O. (1975). Thermal conductivity of soils, PhD thesis, CRREL draft translation 637, 1977, Norwegian University of Science and Technology, Trondheim, Norway.

Jonscher, A.K. (1977). The universal dielectric response, *Nature*, **267 (5613)**, 673-679.

Kersten, M.S. (1949). Thermal properties of soils, Bulletin 28, Engineering Experiment Station, Minneapolis: University of Minnesota.

Kluitenberg, G.J., Ham, J.M., and Bristow, K.L. (1993). Error analysis of the heat pulse method for measuring soil volumetric heat capacity, *Soil Science Society of America Journal*, **57**, 1444-1451.

Landau, L.L., and Lifschitz, E.M. (1985). *Elektrodynamik der Kontinua*, Lehrbuch der Theoretischen Physik, Vol. 8., 5th Ed., Akademie-Verlag, Berlin, Germany.

Lauer, K., Wagner, N., and Felix-Henningsen, P. (2012). A new technique for measuring broadband dielectric spectra of undisturbed soil samples, *European Journal of Soil Science*, **63 (2)**, 224-238.

Lichtenecker, K., and Rother, K. (1931). Die Herleitung des logarithmischen Mischungs-gesetzesaus allgemeinen Prinzipien der stationären Strömung, *Physikalische Zeitschrift*, **32**, 255-260.

Lu, S., Ren, T., Gong, Y., and Horton, R. (2007). An improved model for predicting soil thermal conductivity from water content at room temperature, *Soil Science Society of America Journal*, **71 (1)**, 8-14.

Sepaskhah, A.R., and Boersma, L. (1979). Thermal conductivity of soils as a function of temperature and water content, *Soil Science Society of America Journal*, **43 (3)**, 439-444.

Topp, G.C., Davis, J.L., and Annan, A.P. (1980). Electromagnetic determination of soil water content: measurements in coaxial transmission lines, *Water Resources Research*, **16**, 574-582.

Wagner, N., Emmerich, K., Bonitz, F., and Kupfer, K. (2011). Experimental investigations on the frequency and temperature-dependent dielectric material properties of soil, *IEEE Transactions on Geoscience & Remote Sensing*, **49 (7)**, 2518-2530.

Wagner, N., and Scheuermann, A. (2009). On the relationship between matric potential and dielectric properties of organic free soils: a sensitivity study, *Canadian Geotechnical Journal*, **46 (10)**, 1202-1215.

Wagner, N., Schwing, M., and Scheuermann, A. (2014). Numerical 3D FEM and experimental analysis of the open-ended coaxial line technique for microwave dielectric spectroscopy on soil, *IEEE Transaction on Geoscience and Remote Sensing*, **52 (2)**, 880-893.